24th INTERNATIONAL CONGRESS ON SOUND AND VIBRATION
23–27 July 2017, London

PREDICTION OF IMPACT SOUND INSULATION WITH A HYBRID FINITE ELEMENT-STATISTICAL ENERGY ANALYSIS APPROACH

Pengchao Wang, Arne Dijckmans[1], Geert Lombaert and Edwin Reynders
KU Leuven, Dept. of Civil Engineering, Kasteelpark Arenberg 40, B-3001 Leuven, Belgium
email: pengchao.wang@kuleuven.be

The impact sound insulation quality of floors is vital for the acoustic comfort in buildings. Although impact sound insulation can be experimentally assessed, a numerical prediction tool is important for design and optimization purposes. The development of such a prediction tool is challenging, because of the difficulties in predicting the impact force and the dynamic response of building elements, the quantification of the sound radiation from the floor, and coupling effects between the floor and other parts of the building. In this contribution, the impact force produced by a tapping machine is predicted by a conventional impact model. To predict the impact sound radiation at medium and high frequencies, a decoupled hybrid approach is developed to model the floor and the receiving room. The floor is deterministically modeled with finite elements (FE) and the radiated sound power is obtained by integrating the sound intensity over the vibrating floor surface. The receiving room is modeled as a pure-tone diffuse reverberant field using statistic energy analysis (SEA), and the sound pressure level in the room is then determined by a rigorous power balance within the decoupled floor-room system. This approach is applied to predict the impact sound level in a receiving room under a concrete floor, and the result shows good agreement with measurements at medium and high frequencies.
Keywords: impact sound insulation, numerical prediction, hybrid FE-SEA approach

1. Introduction

The impact sound insulation of a floor structure is required to ensure the acoustical comfort in engineering applications. Laboratory measurements are indispensable to assess the impact sound insulation of an existing floor structure. A numerical prediction tool, however, is required for design and optimization of new floors.

To generate a complete prediction tool of impact sound insulation, the knowledge of the input impact force is required. To produce repetitive impact force and rate the impact sound level, standardized sources are often used such as the standard tapping machine (STM) according to ISO 10140 [1]. Depending on the type of floor, the description of the STM impact force ranges from basic impact scenario [2], to the specific consideration of interaction between an impact hammer and an excited floor structure, e.g. [3]. Furthermore, a fully deterministic numerical model, e.g., using the finite element (FE) method, to analyze the vibro-acoustic response at medium and high excitation frequencies confronts two challenges. First, the decreasing wavelengths of system deformation require increasing number of degrees of freedom (DOFs) to capture the complex response pattern, which is computationally demanding [4]. Second, the local response is considerably sensitive to wave scattering caused

[1]currently at: Belgian Building Research Institute, Av. Pierre Holoffe 21, B-1342 Limelette, Belgium.

by random system properties, such as the spatial variation in geometry, material properties and boundary conditions [5]. In order to overcome these difficulties, a hybrid strategy given in [6], [7] and [8] has been proposed to model the vibro-acoustic system. In this strategy the floor is modeled in full detail with FE, while the acoustical system is stochastically modeled as a random diffuse field using statistical energy analysis (SEA). This paper presents a complete tool to predict the sound pressure level (SPL) in the receiving room under a floor excited by a STM. For typical heavyweight floors, the floor-room coupling is regarded as weak or negligible to affect the vibro-acoustic response [9], and therefore is disregarded.

The paper is organized as follows. In Section 2, the impact model and the hybrid FE-SEA model are presented. In Section 3, a case study is given to validate this prediction tool. Conclusions are given in Section 4.

2. Methodology

2.1 Impact model

The ISO STM consists of five cylindrical hammers, with mass of $m = 0.5$ kg. Each hammer impacts the floor surface after a free fall from a height $h = 4$ cm. The interval between each two impacts is $T = 0.1$ s. The impact model in [2] assumes that the floor structure is infinitely stiff and therefore the contact time per impact is extremely short. Disregarding the hammer rebound, the periodic impact signal of infinite time length is subsequently decomposed in a Fourier series at any excitation $n/T,\ n \in \mathbb{N}$, such that

$$\hat{f}_n \approx \frac{2mv_0}{T} \tag{1}$$

where $v_0 = \sqrt{2gh}$, with g the acceleration of gravity. As the impact signal is periodical, the power spectral density (PSD) of the impact signal is taken to be uniformly distributed over frequency domain, instead of nonzero only at excitation frequencies. Therefore $S_{f,\mathrm{rms}} = f_{\mathrm{rms}}^2/f_0 = 3.92\ \mathrm{N}^2/\mathrm{Hz}$ [2]. Integrating the impact PSD over 1/1 and 1/3 octave bands gives the corresponding squared RMS force spectrum, as shown in Fig. 1. A rough prognosis of the total normalized SPL over a frequency band is given regarding on a STM excited isotropic floor, such that [2]

$$L_{\mathrm{n,\Delta f}} = 10 \log \frac{\sigma \rho_0 c B}{\pi \eta m'' \sqrt{D m''} A_0 W_0} \tag{2}$$

where B equals to 0.71 and 0.23 for 1/1 and 1/3 octave bands, respectively. η, m'' and D are the radiation efficiency, damping loss factor, surface density and bending stiffness of the floor. σ is the frequency dependent sound radiation efficiency of the floor and can be roughly determined using an approach of Cremer [10]. ρ_0 and c are the air density and sound speed in air, respectively. $A_0 = 10\ \mathrm{m}^2$ and $W_0 = 1 \times 10^{-12}$ W the reference room absorption area and sound power.

2.2 Hybrid FE-SEA approach

2.2.1 The decoupled FE-SEA system

A 'floor-room' system of interest is simulated using a hybrid approach for the prediction of impact sound insulation. As shown in Fig. 2, the floor is deterministically modeled using FE, while the room is considered as a superposition of a deterministic direct field and a random reverberant field, and modeled by SEA. The equation of motion for this decoupled floor is written as

$$\mathbf{D}_{\mathrm{d}}\mathbf{u} = \mathbf{f} \tag{3}$$

where $\mathbf{D}_{\mathrm{d}} \in^{N_{\mathrm{dof}} \times N_{\mathrm{dof}}}$ is the dynamic stiffness matrix of the deterministic floor, $\mathbf{u} \in^{N_{\mathrm{dof}}}$ and $\mathbf{f} \in^{N_{\mathrm{dof}}}$ are the vectors of displacements and external forces, with N_{dof} the number degrees of freedom (DOFs) of the floor. The cross-spectrum of floor displacements is written as

$$\mathbf{S}_{uu} = \mathbf{u}\mathbf{u}^{\mathrm{H}} = (\mathbf{D}_{\mathrm{d}}^{-1}\mathbf{f})(\mathbf{f}^{\mathrm{H}}\mathbf{D}_{\mathrm{d}}^{-\mathrm{H}}) = \mathbf{D}_{\mathrm{d}}^{-1}\mathbf{S}_{ff}\mathbf{D}_{\mathrm{d}}^{-\mathrm{H}} \tag{4}$$

where $\mathbf{S}_{uu}$ and $\mathbf{S}_{ff}$ are the power spectrums of displacements and external forces at the floor DOFs, respectively. The notation $.^{\mathrm{H}}$ denotes the Hermitian transpose, i.e., $\mathbf{u}^{\mathrm{H}} = \mathbf{u}^{*\mathrm{T}}$.

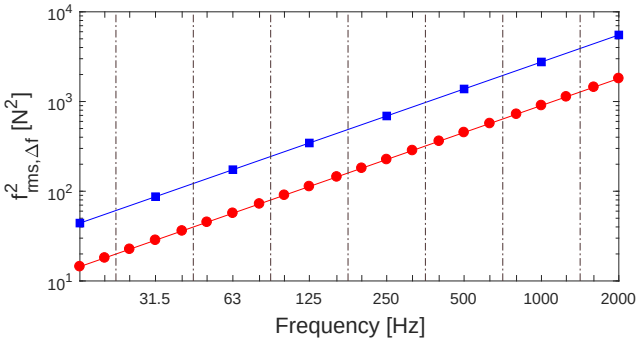

Figure 1: The squared RMS force spectrum in 1/1 octave bands (square) and 1/3 octave bands (circle). Dashed lines are the bounds between adjacent bands.

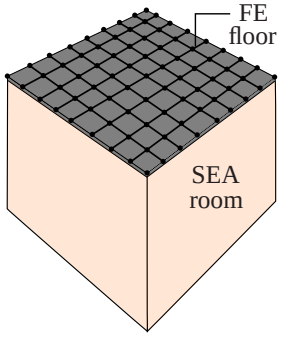

Figure 2: A 'floor-room' system is modeled by FE method and SEA.

2.2.2 *Impact sound radiation from a floor structure*

For a point-excited floor panel in an infinite baffle is point-excited, the overall sound power P_{rad} radiated to an adjacent half-space can be estimated by integrating the sound intensity over the vibrating planar surface [11], such that

$$P_{\mathrm{rad}} = \frac{1}{2}\int_S \mathrm{Re}\{v(x,y)^* p(x,y)\}dxdy = \frac{\omega}{2}\int_S \mathrm{Im}\{u(x,y)^* p(x,y)\}dxdy \tag{5}$$

where $v(x,y) = i\omega u(x,y)$ is the magnitude of the harmonic velocity at coordinate (x,y) of the floor. $p(x,y)$ is the magnitude of the sound pressure, which can be computed as the Rayleigh integral as

$$p(x,y) = -\frac{\omega^2\rho_0}{2\pi}\int_S u(x',y')\frac{\exp(-ik_a r)}{r}dx'dy' \tag{6}$$

where $k_a = \omega/c$ is the acoustic wavenumber in the air. r is the distance between the impact point (x',y') and observation point (x,y). This deterministic expression refers to the mean surface pressure field, as the random effects from reverberant field are assumed to be zero mean. Inserting Eq. (6) into (5) gives the mean radiated power as

$$P_{\mathrm{rad}} = \frac{\omega}{2}\left(-\frac{\omega^2\rho_0}{2\pi}\right)\int_S\int_S u(x,y)^* u(x',y')\mathrm{Im}\left\{\frac{\exp(-ik_a r)}{r}\right\}dx'dy'dxdy \tag{7}$$

In discretized form, this expression becomes:

$$P_{\mathrm{rad}} = \frac{\omega}{2}\mathrm{Im}\{\mathbf{u}^{\mathrm{H}}\mathbf{D}_{\mathrm{dir}}\mathbf{u}\} = \frac{\omega}{2}\sum_{rs}\mathrm{Im}\{D_{\mathrm{dir},rs}\}S_{\hat{u}\hat{u},rs} = \frac{\omega}{2}\sum_{rs}\mathrm{Im}\{D_{\mathrm{dir},rs}\}\left(\mathbf{D}_{\mathrm{d}}^{-1}\mathbf{S}_{ff}\mathbf{D}_{\mathrm{d}}^{-\mathrm{H}}\right)_{rs} \tag{8}$$

where $\mathbf{D}_{\mathrm{dir}} \in^{N_{\mathrm{dof}} \times N_{\mathrm{dof}}}$ is the dynamic stiffness matrix of the direct field of the room, as seen from the plate. The entry $D_{\mathrm{dir},rs}$, representing the acoustic load along the r-th DOF required to generate a unit response along the s-th DOF, is expressed as

$$D_{\mathrm{dir},rs} = \left(\frac{-\omega^2\rho_0}{2\pi}\right)\frac{\exp(-ik_a r_{rs})}{r_{rs}}\Delta x_r \Delta y_r \Delta x_s \Delta y_s \tag{9}$$

where Δx_r and Δy_r, e.g., are dimensions of tributary mesh area for the node with the r-th DOF.

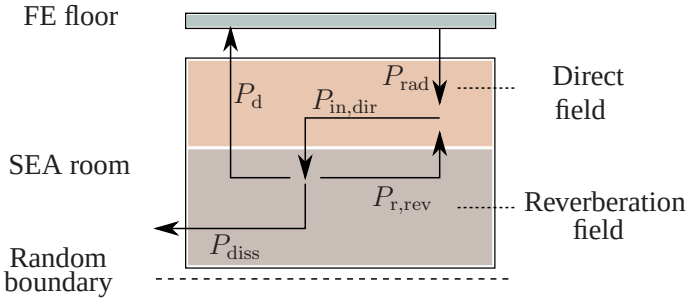

Figure 3: The power flows within the FE-SEA system.

2.2.3 SPL in the adjacent room

The sound power flow within the FE-SEA system is presented in Fig. 3. The input power in the direct field, $P_{\mathrm{in,dir}}$, consists not only of the radiated power P_{rad} from the excited floor, but also of the power flowed from the reverberation field $P_{\mathrm{r,rev}}$, so that

$$P_{\mathrm{in,dir}} = P_{\mathrm{rad}} + P_{\mathrm{r,rev}} \tag{10}$$

The input power $P_{\mathrm{in,dir}}$ flows to the reverberant field, and then either flows back to the direct field or the floor, or is dissipated within the reverberant field, so that

$$P_{\mathrm{in,dir}} = P_{\mathrm{r,rev}} + P_{\mathrm{d}} + P_{\mathrm{diss}} \tag{11}$$

in which P_{diss} and P_{d} are described as [7]

$$\begin{aligned} P_{\mathrm{d}} &= \omega\eta_{\mathrm{d}}\hat{E} \\ P_{\mathrm{diss}} &= \omega\eta_{\mathrm{rev}}\hat{E} \end{aligned} \tag{12}$$

where $\hat{E}$ and η_{rev} are the average sound energy and damping loss factor within the reverberation field. η_{d} is the coupling loss factor between the floor and room, which can be expressed as [7]

$$\omega\eta_{\mathrm{d}} = \frac{2}{\pi n_{\mathrm{m}}}\sum_{rs}\mathrm{Im}\{\mathbf{D}_{\mathrm{d}}\}_{rs}\left(\mathbf{D}_{\mathrm{d}}^{-1}\mathrm{Im}\{\mathbf{D}_{\mathrm{dir}}\}\mathbf{D}_{\mathrm{d}}^{-\mathrm{H}}\right)_{rs} \tag{13}$$

where n_{m} is the modal density of the room. Using Eqs. (10) to (12) the equilibrium of power flows within the FE-SEA system is given as

$$\omega(\eta_{\mathrm{rev}} + \eta_{\mathrm{d}})\hat{E} = P_{\mathrm{rad}} \tag{14}$$

The normalized impact SPL in the receiving room is determined as

$$L_{\mathrm{n}} = 10\log\frac{p_{\mathrm{eff}}^2}{p_0^2} + 10\log\frac{A}{A_0} = 10\log\frac{\hat{E}\rho_a c^2}{V p_0^2} + 10\log\frac{A}{A_0} \tag{15}$$

in which p_{eff}^2 is the square of spatial averaged effective sound pressure, A and V the absorption area and volume of the receiving room, and $p_0 = 2\times10^{-5}$ Pa the reference sound pressure.

3. Validation

3.1 Description of the floor structure and experimental modal analysis

A concrete floor of dimensions $2.2 \times 2.2 \times 0.1$ m^3, density $\rho = 2300$ kg/m^3, Young's modulus $E = 30$ GPa and Poisson's ratio $\nu = 0.33$ is studied. This floor is suspended in the opening between two transmission rooms via eight bolts, as shown in Fig. 4a. The external floor frame has a thickness of 0.38 m, and an irregular shape as shown in Fig. 4b.

(a) (b)

Figure 4: The concrete floor between two transmission rooms: (a) the upper and lower surface of the suspended concrete floor. The bolts are indicated by circles. (b) the top view of the full floor. The dimensions are in meter.

In order to investigate the modal behavior of the floor, a roving hammer test was performed, in which the floor was excited by a hammer at 81 different positions, and the response of the floor was measured with accelerometers at five fixed positions. The data were processed and a modal analysis performed using MACEC, a MatLab toolbox for experimental and operational modal analysis [13]. The identified modal characteristics of the first five modes are shown in Fig. 5.

3.2 FE model and updates

A FE model of the floor was constructed with ANSYS. The suspended floor was modeled with 3D solid elements (of SOLID45 type), while the external part was regarded as infinitely stiff and therefore not considered. Each bolt is modeled as a spring using COMBIN14 element, and the elastic stiffness of a bolt, 128 MN/m, is adopted as the stiffness of each spring. The mesh of this model is given in Fig. 6. The simulated modes are partly inconsistent with the identified ones given in Fig. 5. Although some identified mode shapes are well predicted, the natural frequencies are significantly overestimated, especially the first natural frequency, which is 40 % larger than the identified one (44.51 Hz in Fig. 5a).

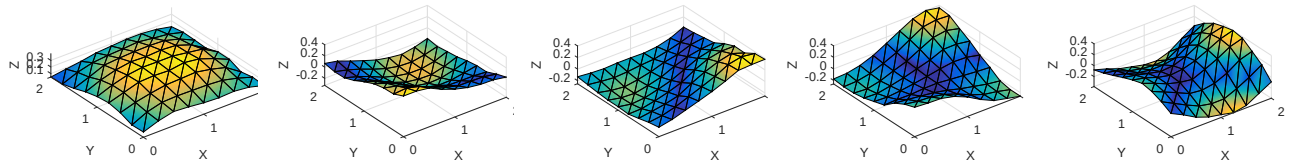

(a) 44.51 Hz (b) 78.91 Hz (c) 84.35 Hz (d) 118.72 Hz (e) 142.53 Hz

Figure 5: Natural frequencies and mode shapes of the first five identified modes of the suspended concrete floor.

The overestimation of the first several natural frequencies may have been caused by the fact that the external floor was assumed as infinitely stiff. This was verified by an updated FE model in which

the external floor frame was simulated as a cantilever structure using 3D SOLID45 elements, as shown in Fig. 7. The first simulated natural frequency was 47.95 Hz, which nearly corresponds with the identified value. Moreover, the dynamic behavior of the floor may also be affected by different pretension status of the bolts. Talking these two aspects into consideration, as well as the lack of information regarding the pretension status of each bolt, the small suspended floor model in Fig. 6 was readopted as the final model, while the stiffnesses of boundary bolts were calibrated to meet the identified modal characteristics in Fig. 5. The calibrated bolt stiffness is decreased to 31.7 MN/m, which compensates for the flexibility of the external floor. The first five updated natural frequencies and mode shapes are given in Fig. 8.

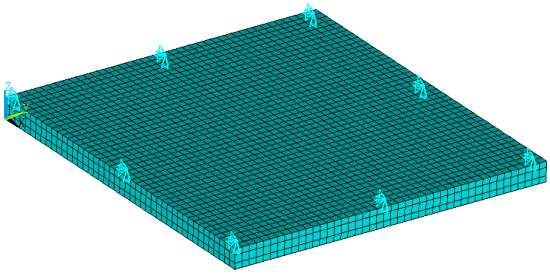

Figure 6: Finite element mesh. The suspended floor is modeled with 3D solid elements, and the bolts are modeled as spring elements.

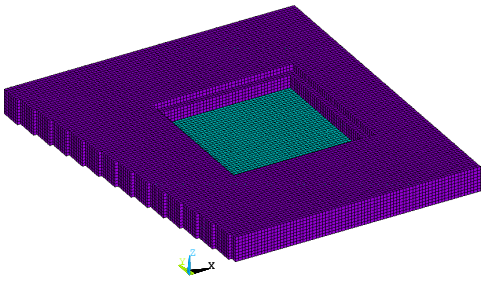

Figure 7: Finite element mesh. Both the suspended floor and the external frame are modeled with 3D solid elements, and the bolts are modeled as spring elements.

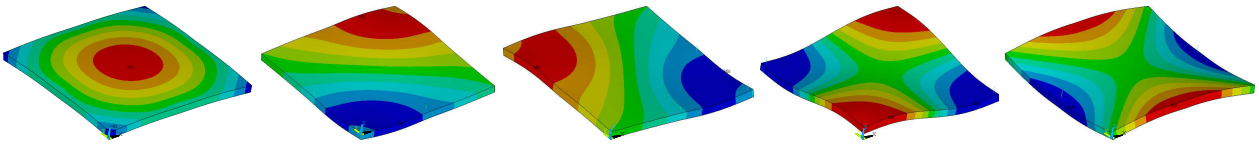

(a) 48.58 Hz (b) 83.94 Hz (c) 83.94 Hz (d) 111.62 Hz (e) 126.71 Hz

Figure 8: Natural frequencies and mode shapes of the first five simulated modes of the suspended concrete floor.

3.3 Floor response and receiving room SPL

Based on the developed FE model, the floor response and the SPL in the receiving room can be numerically predicted, and then validated by means of measurements. First, the frequency response function (FRF), representing the response (e.g., displacement, velocity or acceleration) along a DOF due to the unit load along another DOF, is computed using the modal summation approach. The input modal damping loss factors below and above 300 Hz are determined by the foregoing modal identification and a structural reverberation test, respectively. Alternatively, the FRF matrix can be constructed by invoking the principle of reciprocity on the result of the roving hammer test. The numerically and experimentally determined FRFs of accelerations for three randomly selected pairs of exciting and observing DOFs are plotted in Fig. 9. The overall trend and magnitude of the two results match relatively well, while the discrepancies at resonances are present, indicating the errors of damping loss measurement and modal simulation.

A measurement of the receiving room SPL was performed in accordance with the ISO 10140 standard [1], with the exception that the measured SPL was also averaged over 1/48-octave bands instead of 1/3-octave bands to obtain a finer frequency resolution. The STM excitations were given at eight random positions over the floor area. For each position the STM was placed at a random orientation (see Fig. 10), and the sound level is sampled at eight random microphone locations in

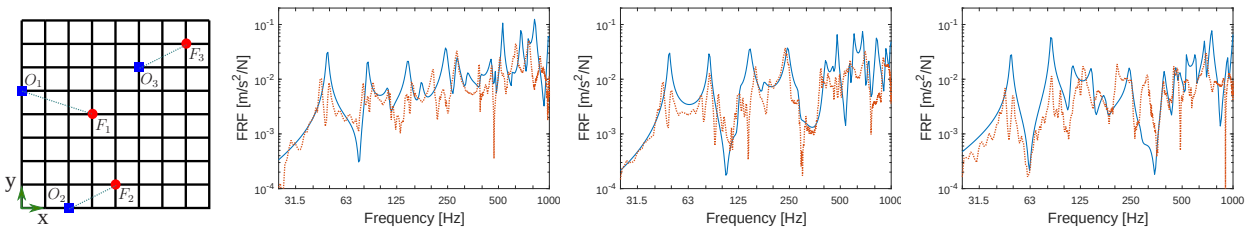

(a) DOF pairs (b) $F_1 - O_1$ (c) $F_2 - O_2$ (d) $F_3 - O_3$

Figure 9: The locations of three randomly selected pairs of exciting and observing DOFs (a). FRFs of accelerations regarding DOF pairs in order (b - d). Solid line: simulation. Dotted line: experiment.

the receiving room. Besides, each excitation is simulated and the resultant receiving room SPL is computed using the tool in Section 2. As the dimensions of the STM are much smaller than the horizontal dimensions of the floor, the impacts in period of T are assumed to act at a single location corresponding to the central hammer of the STM (see Fig. 11).

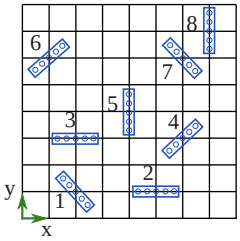

Figure 10: Eight randomly arranged excitation positions and STM orientations.

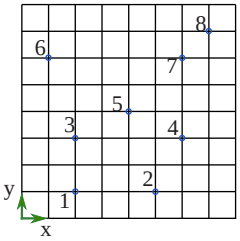

Figure 11: A STM at each excitation location is simplified as its central hammer.

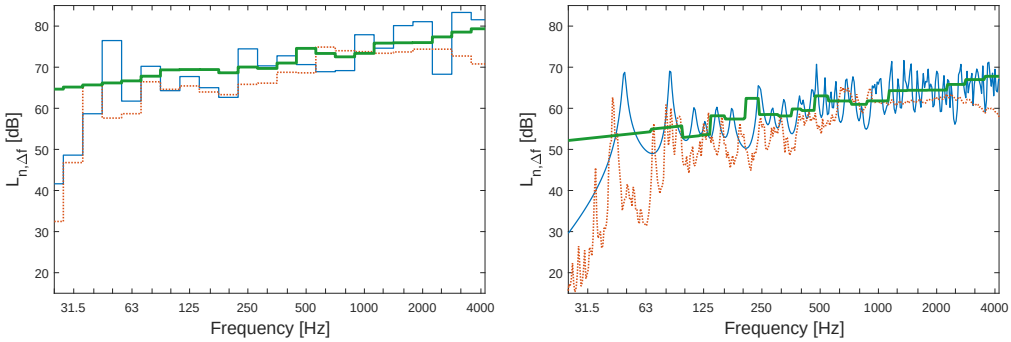

(a) (b)

Figure 12: The normalized SPLs integrated over 1/3-octave band (a) and 1/48-octave band (b). Thin line: hybrid approach. Dotted line: measurement. Thick line: prognosis using model of Beranek and Vér.

In Fig. 12, the normalized SPL averaged over all excitation locations and microphone positions, in both 1/3 and 1/48 octave bands, are given by the measurement and the hybrid approach. A prognosis using Eq. (2) is also presented. The agreement between the measurements and the hybrid predictions is generally good, except around 50 Hz where the SPL is strongly overestimated. This is due to the modal behavior of this particular room, which is disregarded in the model. At higher frequencies, the sound field in the room becomes diffuse, and the accuracy of the hybrid predictions is ensured. Moreover, above 3000 Hz the measured normalized SPL is slightly decreased, which indicates that the assumed infinitely short impact, adopted in the hybrid approach and the prognosis, is inappropriate in this frequency range.

4. Conclusion

This work presents a hybrid approach for the prediction of impact sound insulation at medium and high frequencies. Confronting the challenges in vibro-acoustic analysis at medium and high frequencies, the hybrid FE-SEA approach accounts for local uncertainties of the room and provides robust prediction of impact SPL in the receiving room. This hybrid approach is applied to predict the SPL in a room under a STM excited concrete floor. The agreement with measured values is generally good, except at low frequencies where individual room modes dominate the response, as expected.

REFERENCES

1. ISO 10140:2010: Acoustics - Laboratory measurement of sound insulation of building elements.
2. Beranek, L. L. and Vér, I. L., *Noise and vibration control engineering - principles and applications*, John Wiley & Sons, Hoboken, NJ, (1992).
3. Brunskog, J. and Hammer, P., The interaction between the ISO tapping machine and lightweight floors, *Acta Acustica united with Acustica*, **89** (2), 296-308, (2003).
4. Langley R. S. and Bremner P., A hybrid method for the vibration analysis of complex structural-acoustic systems, *Journal of the Acoustic Society of America*, **105** (3), 1657-1671, (1999).
5. Kompella, M. S. and Bernhard R. J., Variation of structural-acoustic characteristics of automotive vehicles *Noise Control Engineering Journal*, **44**, 93-99, (1996).
6. Shorter, P. J. and Langley R. S., Vibro-acoustic analysis of complex systems, *Journal of Sound and Vibration*, **288** (3), 669-699, (2005).
7. Langley, R. S. and Cordioli, J. A., Hybrid deterministic-statistic analysis of vibro-acoustic systems with domain couplings on statistical components, *Journal of Sound and Vibration*, **321** (3), 893-912, (2009).
8. Reynders, E., Langley R. S., Dijckmans A.and Vermeir G., A hybrid finite element-statistical energy analysis approach to robust sound transmission modeling, *Journal of Sound and Vibration*, **333** (19), 4621-4636, (2014).
9. Fahy, F. J. and Gardonio, P., *Sound and structural vibration: radiation, transmission and response*, Academic press, Oxford, UK, (2007).
10. Cremer, L., Heckl, M. Petersoon B. A. T., *Structure-Borne Sound: structural vibrations and sound radiation at audio frequencies*, Springer, Berlin, (2010).
11. Williams, E. G. and Maynard, J. D., Numerical evaluation of the Rayleigh integral for planar radiators using the FFT, *Journal of the Acoustical Society of America*, **72** (6), 2020-2030, (1982).
12. Langley, R. S., A general derivation of the statistical energy analysis equations for coupled dynamic systems, *Journal of Sound and Vibration*, **135** (3), 499-508, (1989).
13. Reynders, E., Schevenels, M., and De Roeck, G., Technical Report BWM- 2014-06, MACEC 3.3: a Matlab toolbox for experimental and operational modal analysis, (2014).